Gene therapy for Parkinson's disease: preclinical evaluation of optimally configured TH:CH1 fusion for maximal dopamine synthesis

Romina Aron Badin, Katie Binley, Nadja van Camp, Caroline Jan, Jeanne Gourlay, Camille Robert, Pauline Gipchtein, Audrey Fayard, Hannah Stewart, G Scott Ralph, et al.

Molecular Therapy
Methods & Clinical Development
Original Article

Gene Therapy for Parkinson's Disease: Preclinical Evaluation of Optimally Configured TH:CH1 Fusion for Maximal Dopamine Synthesis

Romina Aron Badin,[1,2,7] Katie Binley,[3,7] Nadja Van Camp,[1,2] Caroline Jan,[1,2] Jeanne Gourlay,[1,2] Camille Robert,[1,2] Pauline Gipchtein,[1,2] Audrey Fayard,[1,2] Hannah Stewart,[3] G. Scott Ralph,[3] Yatish Lad,[3] Michelle Kelleher,[3] Julie Loader,[3] Koichi Hosomi,[4,5] Stéphane Palfi,[4,5,6] Kyriacos A. Mitrophanous,[3,6] and Philippe Hantraye[1,2,6]

[1]CEA, DRF, Institute of Biology François Jacob, Molecular Imaging Research Center (MIRCen), 92265 Fontenay-aux-Roses, France; [2]CNRS, CEA, Paris-Sud University, Université Paris-Saclay, Neurodegenerative Diseases Laboratory (UMR9199), 92265 Fontenay-aux-Roses, France; [3]Oxford Biomedica, Windrush Court, Transport Way, Oxford OX4 6LT, UK; [4]AP-HP, Groupe Hospitalier Henri-Mondor, DHU PePsy, Neurochirurgie, Créteil, 94010, France; [5]Université Paris 12, Faculté de Médecine, IMRB, INSERM U955, Team 14, Créteil 94010, France

A recent phase I-II, open-label trial of ProSavin, a lentiviral vector delivering the key enzymes in the dopamine biosynthetic pathway to non-dopaminergic striatal neurons, demonstrated safety and improved motor function in parkinsonian patients. However, the magnitude of the effect suggested that optimal levels of dopamine replacement may not have been achieved. OXB-102, a lentiviral vector with an optimized expression cassette for dopamine biosynthesis, has been shown to achieve a significantly higher dopamine yield than ProSavin. We assessed the efficacy of OXB-102 in the MPTP macaque model of Parkinson's disease (PD). At 6 months post-vector administration, all treated animals showed significant improvements in clinical scores and spontaneous locomotor activity compared to controls, with the highest recovery observed in the OXB-102 high-dose (HD) group. Positron emission tomography quantification of 6-[^{18}F]-fluoro-L-m-tyrosine uptake showed a significant increase in amino acid decarboxylase activity for all treated animals, compared with controls, where the OXB-102 HD group showed the highest level of dopaminergic activity. A toxicology study in macaques demonstrated that the vector was safe and well tolerated, with no associated clinical or behavioral abnormalities and no immune response mounted against any transgene products. Overall, these data support the further clinical development of OXB-102 for the treatment of PD.

INTRODUCTION

Parkinson's disease is a neurodegenerative disorder that gives rise to motor symptoms such as tremor, bradykinesia, rigidity, and postural instability and non-motor symptoms such as anosmia, constipation, apathia, insomnia, and depression.[1–4] The disease is caused by the progressive degeneration of dopaminergic neurons in the substantia nigra pars compacta, leading to a deficiency of dopamine release in the striatum.[5,6] At present, and despite decades of research, the etiology of the disease is still unknown, and preventive or long-term disease-modifying treatments are not currently available. Oral dopamine replacement therapies provide the current standard of care for treating motor symptoms and are highly effective in early- to mid-stage disease.[7–9] However, as the disease progresses, the beneficial effects of these oral therapies decline, and this is combined with the onset of drug-related side effects, such as dyskinesias, and off-target non-motor symptoms.[9–11] In addressing the complications associated with oral therapies, strategies aimed at providing a continuous and local restoration of dopamine to the striatum offer an attractive alternative.[9,12]

A number of gene therapy approaches have been tested in pre-clinical models and early-stage clinical trials of PD patients over the past 20 years.[13,14] Such approaches included stereotaxic delivery of adeno-associated virus (AAV) vectors expressing neuroprotective factors, such as glial-cell-derived neurotrophic factor (GDNF) and neurturin, aimed at slowing the degeneration of dopaminergic neurons,[15–19] and normalization of basal ganglia outputs by delivering expression of glutamate decarboxylase (GAD) to the subthalamic nucleus.[20,21] Despite showing initial promise, neither of these approaches translated into sufficient clinical benefit in sham-surgery-controlled trials.[18,19,21]

More recently, ProSavin a lentiviral vector-based dopamine replacement strategy, was evaluated in pre-clinical and clinical studies.[12,22,23] ProSavin was designed to create dopamine "factories" in non-dopaminergic striatal neurons of the sensorimotor putamen by delivering the three key enzymes in the dopamine biosynthesis pathway: tyrosine hydroxylase (TH), amino acid decarboxylase (AADC), and GTP-cyclohydrolase-1 (CH1).[22] A pre-clinical study in

Received 19 November 2018; accepted 8 July 2019;
https://doi.org/10.1016/j.omtm.2019.07.002.

[6]These authors contributed equally to this work.

[7]These authors contributed equally to this work.

Correspondence: Kyriacos A. Mitrophanous, PhD, Oxford Biomedica, Windrush Court, Transport Way, Oxford OX4 6LT, UK.
E-mail: k.mitrophanous@oxb.com

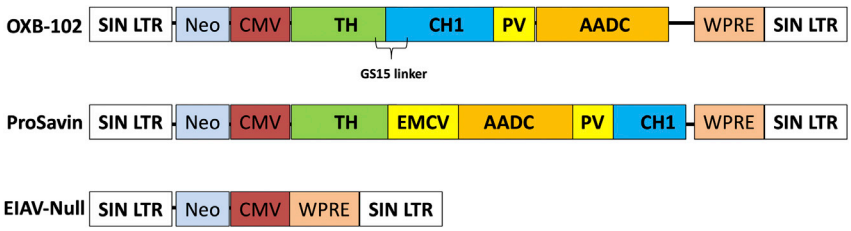

Figure 1. Schematic Diagram showing the Genetic Structure of the Integrated OXB-102, ProSavin, and EIAV-Null Vectors Used in this Study

The OXB-102 vector genome is similar to that of ProSavin, but the order of the three transgenes is different, and OXB-102 encodes a gene fusion of *TH* and *CH1*. ProSavin contains an encephalomyocarditis virus (EMCV) IRES between the *TH* and *AADC* transgenes. The EIAV-Null vector does not encode any transgenes. SIN LTR, self-inactivating long-term repeat; *Neo*, neomycin open reading frame; CMV, cytomegalovirus promoter; *AADC*, amino acid decarboxylase. GS15 linker, a short glycine-serine-rich peptide linker; WPRE, woodchuck posttranscriptional response element; PV, poliovirus IRES.

the 1-methyl-4-phenyl-1,2,3,6-tetrahydropyridine (MPTP)-lesioned non-human primate model showed normalization of motor function and significantly increased striatal dopamine levels in ProSavin-treated animals compared with controls.[23] Consistent with these findings, a phase I-II clinical trial showed a tolerable safety profile and encouraging indications of motor benefit from ProSavin in mid- to late-stage PD patients.[12] Despite these motor improvements, the clinical data indicate that higher levels of dopamine replacement may be required to maximize the clinical benefit.[12,24,25]

OXB-102 (currently in clinical trials under the name AXO-Lenti-PD), a lentiviral vector with an optimized expression cassette for the three dopamine biosynthesis enzymes, was recently developed.[24] The vector contained a fusion construct between TH and CH1 using a flexible linker sequence (GS15), with expression of AADC downstream of an internal ribosome entry site (IRES) sequence. OXB-102 showed a significantly increased capacity for L-Dopa and dopamine production compared with ProSavin in human primary neurons.[24]

Here, we report the findings from a pre-clinical study that investigates the efficacy, safety, and biodistribution of OXB-102 in non-human primates.

RESULTS

Bilateral Intraputaminal Vector Delivery

Stably parkinsonian primates received bilateral stereotaxic injections of OXB-102 (low-dose [LD] or high-dose [HD]), ProSavin, or Equine Infectious Anaemia Virus (EIAV)-Null vector (Figure 1; Table 1).

MRI at 3 months post-administration demonstrated correct placement of all injection sites within the motor post-commissural putamen (Figure S1), apart from one primate in the ProSavin treatment group, which presented a single injection site that was positioned 2 mm anterior to the anterior commissure in both hemispheres.

Six primates presented a slight hyposignal in the left post-commissural putamen corresponding to a blood deposit or micro-hemorrhage, most likely due to mechanical damage at the time of vector infusion. Five primates presented a similar hyposignal on the right hemisphere. No further abnormalities were detected at the remaining target sites.

Efficacy

Clinical Scores

Following MPTP intoxication, all study animals developed parkinsonian symptoms, with a similar increase in clinical rating scores (CRS) observed across all groups (Figure 2A).

Following vector administration, the EIAV-Null group remained stably parkinsonian, with scores similar to baseline across all time points. For all other treatment groups (ProSavin, OXB-102 LD, OXB-102 HD), progressive improvements in CRS were observed across the 6-month assessment period. All three groups showed significant differences in CRS from the EIAV-Null control group at all time points from 2 to 6 months. A repeated-measures ANOVA demonstrated a significant group effect ($p \leq 0.0001$) and time effect ($p < 0.0001$). A Fisher's least significant difference (LSD) post hoc analysis revealed that all treatment groups were significantly different from the EIAV-Null vector control group (ProSavin, $p = 0.0005$; OXB-102 HD, $p = 0.001$; OXB-102 LD, $p = 0.001$). There were no significant differences in CRS between the OXB-102 HD, OXB-102 LD, and ProSavin treatment groups at any time point.

Locomotor Activity

Video-based quantification of locomotor activity was performed on all animals at baseline, post-MPTP intoxication, and post-vector administration at 3 and 6 months. MPTP treatment resulted in a decrease in mean spontaneous locomotor activity, as assessed by total distance moved (TDM), of at least 90% ± 2% in all treatment groups compared to baseline (Figure 2B). At both time points post-vector administration, all three active treatment groups showed an increase in TDM relative to post-MPTP values, with similar levels of improvement observed in the ProSavin and OXB-102 LD treatment groups. The OXB-102 HD group showed the greatest improvement in mean locomotor activity relative to post-MPTP baseline at both time points (87% ± 1% at 3 months and 91% ± 1% at 6 months). The EIAV-Null vector control group showed no change in locomotor activity compared to post-MPTP baseline activity at 3 months and a decline in locomotor activity at 6 months (-22% ± 6%). A repeated-measures ANOVA examining the differences in locomotor activity

Table 1. Study Groups and Vector Assignment

Treatment Group	Group Size	Total Vector Dose Administered per Animal
Efficacy Study		
EIAV-Null	4	2×10^7 TU
ProSavin	4	1×10^7 TU
OXB-102 LD[a]	4	4×10^6 TU
OXB-102 HD	4	2×10^7 TU
GLP Toxicology Study		
OXB-102	6 (3 male, 3 female)	7×10^6 TU
Buffer	6 (3 male, 3 female)	—

[a]TSSM formulation buffer was used to dilute OXB-102 HD to generate OXB-102 LD.

as a percentage change from post-MPTP values showed a significant group effect ($p = 0.0003$), time effect ($p < 0.0001$), and Time × Group effect ($p < 0.0001$). A LSD post hoc analysis revealed that all treatment groups were significantly different from the EIAV-Null vector control group (ProSavin, $p = 0.001$; OXB-102 LD, $p = 0.002$; and OXB-102 HD, $p < 0.001$).

L-Dopa Challenge

To compare and assess the response to pharmacological dopaminergic stimulation, two L-Dopa challenges were performed: the first before vector administration and after MPTP lesioning and the second at 3 months post-vector administration. At each time point, the change in locomotor activity was calculated relative to data acquired prior to and shortly after L-Dopa challenge. The mean fold increase in locomotor activity following L-Dopa challenge was 9.28 ± 4.35 across all study animals post-MPTP lesioning. At 3 months post-vector administration, the mean fold change post-challenge was significantly reduced to 1.76 ± 0.39 across the three active treatment groups ($p = 0.01$, for all) compared to the post-MPTP stage, indicating that the additional oral L-Dopa had less effect after vector treatment. In the EIAV-Null control group, the mean fold change at 3 months post-challenge was 12.48 ± 6.15, which was not significantly different from the post-MPTP assessment ($p = 0.71$). No behavioral adverse events were observed during L-Dopa challenge in any group.

Positron-Emission Tomography (PET) Imaging

All study animals received a 6-[18F]fluoro-L-m-tyrosine (6-FMT) scan at baseline, post-MPTP lesioning, and at 6 months post-vector administration. Figure 3A shows a representative parametric image of one primate per treatment group at 6 months and representative baseline and post-MPTP scans with the same radioligand prior to vector administration. Quantification of the PET analysis showed a 76% mean reduction in 6-FMT uptake as quantified by Ki in the caudate nucleus and putamen across all primates post-MPTP intoxication, compared to pre-lesion baseline data ($p < 0.0001$, t test). At 6 months, Ki was increased in all active treatment groups and not in the EIAV-Null group relative to post-MPTP values (Figure 3B). A one-way ANOVA showed a significant group effect ($p < 0.0001$).

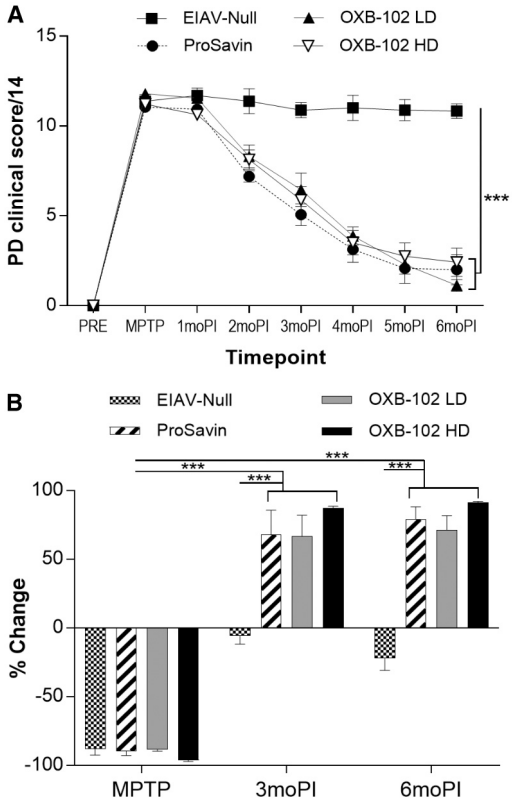

Figure 2. Behavioral Analysis of Animals following MPTP Intoxication and Post-vector Administration

(A) Clinical rating scores. Pre-MPTP score represents baseline data from all study animals prior to randomization into study groups. Subsequent data represent mean scores for each study group from 2 -4 assessments performed at different time points after viral delivery. moPI, months post-injection. (B) EthoVision quantification of the percentage change in TDM following MPTP intoxication and at 3 and 6 months post-viral vector delivery. The percentages were calculated from the last 3 TDM values obtained at each time point. The data are relative to baseline (for post-MPTP) or relative to post-MPTP values (for 3 and 6 moPI). Data represent mean ± SEM. ANOVA ***$p \leq 0.002$.

The relative increase in Ki observed in the OXB-102 HD treatment group was significantly different from that in the EIAV-Null ($p < 0.0001$; LSD post hoc test) and ProSavin ($p < 0.001$; LSD post hoc test) treatment groups at 6 months. The OXB-102 LD vector-treated animals showed a significant difference in relative Ki from the EIAV-Null ($p < 0.0001$; LSD post hoc test) and ProSavin ($p < 0.03$; LSD post hoc test) treatment groups at 6 months. No significant changes in Ki were observed in the non-injected caudate nuclei from any group.

Histology

Immunohistochemical analysis of the vector-injected macaque brains was performed to evaluate transgene expression in the injected putamen. The neuronal tropism of the EIAV vectors was confirmed by co-localization of TH transgene expression with the neuronal marker NeuN in the putamen of animals injected with OXB-102

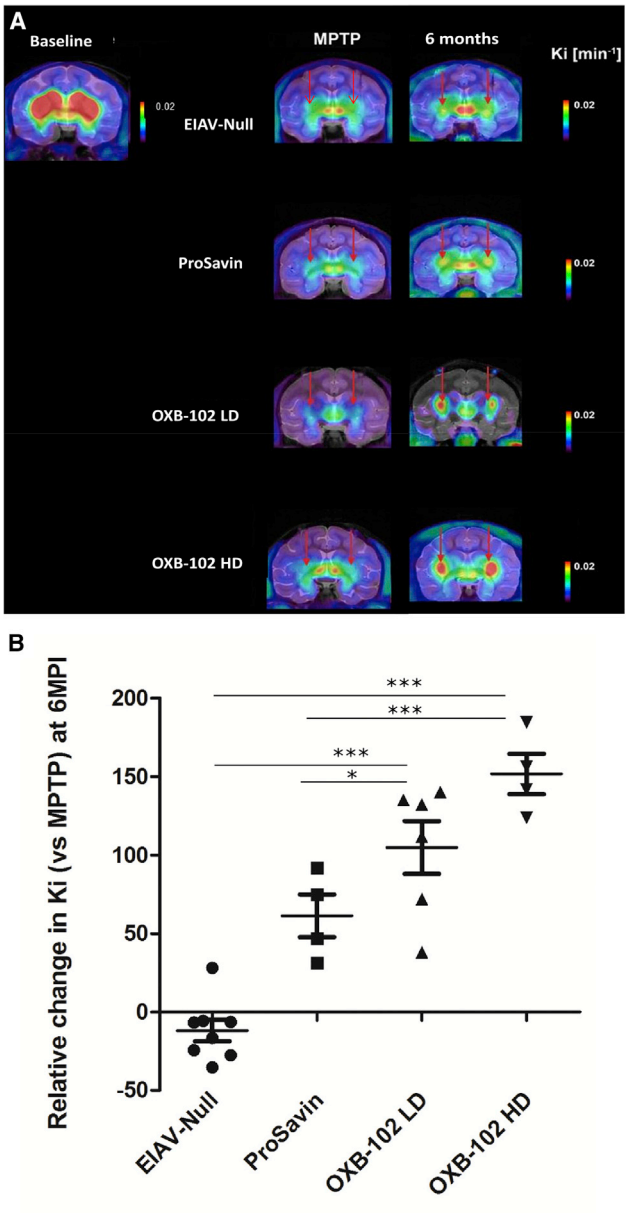

Figure 3. 6-FMT PET Imaging Data

(A) Parametric images showing commissural coronal sections in one representative primate at baseline and then for one representative animal for each treatment group (EIAV-Null, ProSavin, OXB-102 LD, and OXB-102 HD) following MPTP intoxication and at 6 months post-vector administration. Images are presented with scale bars for tracer binding intensity (red indicates highest, and violet indicates lowest). (B) Quantification of 6-FMT binding in all study groups at 6 months post-vector administration relative to post-MPTP data. Data represent mean change ± SEM. ANOVA: *p = 0.05; p ≤ 0.001***

HD (Figure 4A). No co-localization of transgene expression was observed with the astrocyte marker GFAP (Figure 4B). This result was reproduced in all primates injected with ProSavin, OXB-102 LD, and OXB-102 HD (data not shown).

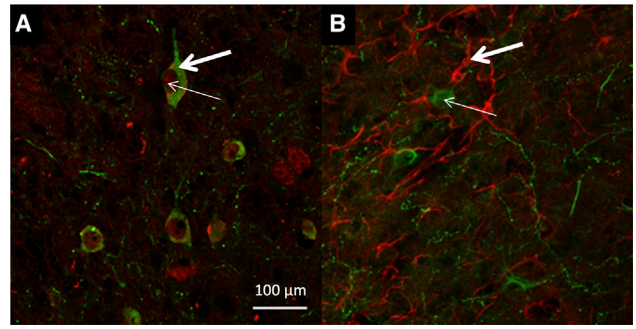

Figure 4. Representative Confocal Images of a Macaque Brain Treated with OXB-102 HD Showing the Neuronal Tropism of the EIAV Vectors

(A) Dual staining for TH (green, bold arrow) and the NeuN neuronal marker (red, thin arrow). (B) Dual staining for TH (green, thin arrow) and the GFAP astrocyte marker (red, bold arrow). Scale bar, 100 µm.

Expression of the three transgene products (TH, AADC, and CH1) was observed in the putamen of all animals receiving ProSavin or OXB-102 around the area of the injection site (Figure 5A). No positive staining for the three transgenes was observed in the putamen of the EIAV-Null controls. Quantification of the transduction volumes suggests a non-significant increase ($p = 0.053$) in TH expression in the OXB-102 HD group compared to the ProSavin or OXB-102 LD group, while no differences in transduction volume were observed for CH1 or AADC (Figure 5B). While co-staining of transgenes in the same section was technically challenging, AADC expression at the protein level was detected in the same striatal cells expressing the *Th* enzyme at the mRNA level (Figure 5C).

Immunogenicity

Baseline and terminal (6 months) serum samples were evaluated for antibody responses against the vector components and the transgene products by western blot analysis (Table 2). Most of the animals (15/16) developed antibodies against VSV-G, and many (10/15) also developed antibodies against the EIAV p26/GagPol. No antibody responses were observed against any of the transgene products (TH, AADC, and CH1).

GLP Toxicology Study

A Good Laboratory Practice (GLP) toxicology study investigated the tolerability of bilateral intrastriatal delivery of OXB-102 vector in normal healthy cynomolgus macaques (Table 1). The vector used for this study was produced using a Good Manufacturing Practice (GMP) manufacturing process. Over the 26-week observation period, OXB-102 was demonstrated to be well tolerated and with no clinical signs or abnormal observations noted. Physical examination and assessment of activity, dyskinesia rating, and behavioral scoring revealed no OXB-102-related effects. Additionally, there were no treatment-related changes in body weight, appetite, ophthalmoscopy, electrocardiogram (ECG), blood pressure, clinical pathology, macroscopic findings, or organ weights. Microscopic findings considered to be related to the treatment of

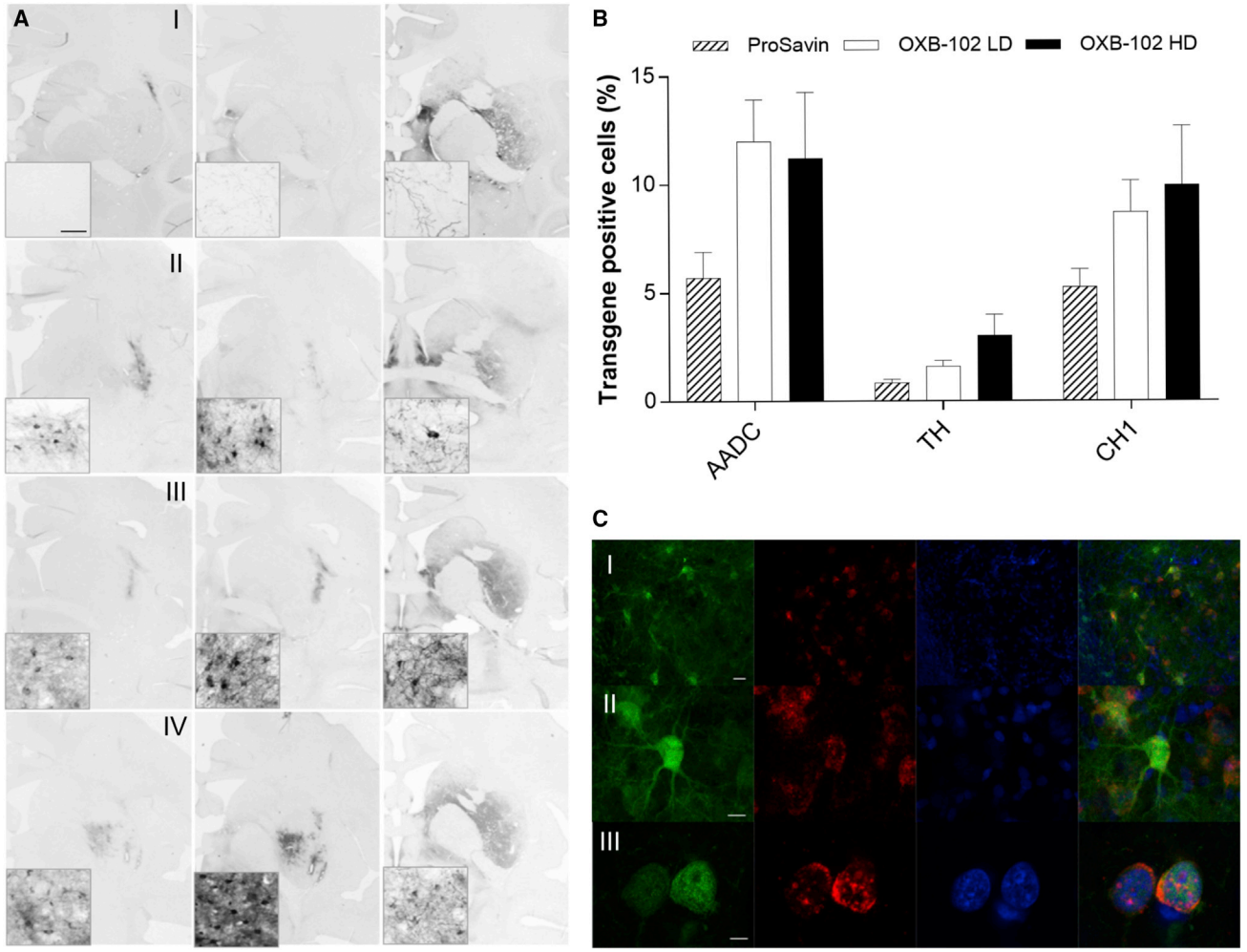

Figure 5. Expression Levels of CH1, AADC, and TH in Transduced Striatal Cells of MPTP NHP

(A) Representative coronal sections showing histochemical staining for CH1 (left column), AADC (middle column), and TH (right column). Coronal brain sections were prepared in study animals 6 months post-vector administration with EIAV-Null (I), ProSavin (II), OXB-102 LD (III), and OXB-102 HD (IV). Scale bar: 50μm. (B) Transduction volumes showing the percentage volume (in cubic millimeters) of TH, CH1, and AADC transgene expression in the putamen of ProSavin, OXB-102 LD, and OXB-102 HD treatment groups. Values are presented as mean ± SEM. (C) Gene expression in striatal cells transduced with OXB-102. Immunohistochemistry showing AADC staining (green) and RNAScope showing mRNA levels of *Th* (red) in the putamen of non-human primates 6 months after OXB-102 injection. DAPI-positive cell nuclei are shown in blue, and colocalization of all markers is shown in the last column. Scale bars: 20 μm (I), 10 μm (II), and 5 μm (III).

OXB-102 were minimal to mild perivascular mononuclear cell infiltration with-without pigmented macrophage infiltration at the injection sites. These were not associated with any systemic observations.

Antibody responses directed against VSV-G were detected at week 4 in all six macaques that received OXB-102 and remained present at week 26 (Table 2; Figure S2). In four of the six OXB-102-treated macaques, p26 responses were also observed, detectable at weeks 13 and 26 in three animals and week 26 in the fourth. An antibody response against a 50- to 60-kDa HEK293T-packaging cell antigen was detected at weeks 13 and 26 in one animal. Responses were not observed against any of the transgene products.

Whole-body biodistribution analysis showed that vector-associated RNA and DNA sequences were not detected in the majority of biological samples from OXB-102-treated animals. Vector-associated DNA sequences were only detected in a small number of samples at a level that was below the lower limit of quantification for the assay (Table 3). Vector particle (RNA) dissemination or persistence in plasma and shedding in cerebrospinal fluid was absent. There was no indication of a consistent or robust presence of vector-associated RNA or DNA sequences.

DISCUSSION

OXB-102 was designed to provide a gene therapy vector with an enhanced capability for dopamine replacement using an optimized

Table 2. Summary of Western Blot Assessments of Antibody Responses in Study Animals

Treatment Group	VSV-G Response	p26 Response	Transgene Product Response
Efficacy Study[a]			
EIAV-Null	4/4	3/4	0/4
ProSavin	4/4	2/4	0/4
OXB-102 LD	3/4	1/4	0/4
OXB-102 HD	4/4	4/4	0/4
GLP Toxicology Study			
OXB-102	6/6[b]	4/6[c]	0/6
Buffer	0/6	0/6	0/6

[a]Responses from end-of-study samples at 6 months post-vector administration.
[b]All responses are from 4 weeks.
[c]Responses are from 13 weeks in 3 animals and 26 weeks for one animal.

Table 3. Summary of PCR Analyses of Samples from Animals in the GLP Safety Study following Intra-striatal Administration of OXB-102

Method and Tissue or Sample Type	Time Point			
	Week 2	Week 4	Week 13	Necropsy
RNA Analysis of Plasma and CSF by qRT-PCR				
Plasma	0/6	—	—	—
CSF				0/6
DNA Analysis of Tissues or Blood Cells by qPCR				
Buffy coat	4/6, NQ < 10[a]	0/6	—	—
Testes (left)				0/3
Ovaries (left)				0/3
Mandibular lymph node				0/5[b]
Cervical lymph node				0/5
Spleen				0/6
Pancreas				0/6
Liver				1/6, NQ < 10
Kidney (left)				0/6
Heart				1/6, NQ < 10
Lung				1/6, NQ < 10
Retina				1/6, NQ < 10
Optic nerve (left)				0/6
Optic nerve (right)				0/6
Cervical spinal cord				2/6, NQ < 10

[a]DNA was detected but was non-quantifiable (NQ) below 10 copies (<10) in 4 out of 6 animals.
[b]No sample was available for 1 animal; therefore, n = 5 for this group.

expression cassette encoding a novel *Th-Ch1* gene fusion.[24] These are the first studies to demonstrate the pre-clinical safety and efficacy of this vector in non-human primates.

Despite encouraging pre-clinical and early-phase clinical studies of gene therapy approaches for PD, none, as yet, have fulfilled their promise in placebo- or sham-surgery-controlled clinical trials.[18,19,21] The reason for this lack of translation to the controlled setting is caused by a number of factors but is largely centered on the marked placebo effect that is often observed in PD clinical trials investigating surgical interventions.[26,27]

A number of AAV-based gene therapies are being developed to treat PD, but due to the limited coding capacity of the AAV vector compared to that of the EIAV lentiviral vector, they are not able to deliver all three dopamine-producing enzymes.[28,29] In an AAV approach currently in clinical trials, one component of OXB-102, the *AADC* gene, is being delivered to the putamen with the aim of increasing the amount of the enzyme that converts levodopa to dopamine in the target brain cells, thereby making levodopa therapy more effective. Similar to ProSavin and OXB-102, this approach has been shown to be safe and well tolerated, with signs of efficacy.[30] Other AAV-based clinical trials involve delivering neuroprotective genes such as neurturin that could protect the dopamine-producing brain cells, thereby slowing or possibly reversing disease progression.[31] Results, to date, have been mixed, but the trials are ongoing.

The previously reported phase I-II clinical study of ProSavin demonstrated that the vector was well tolerated and showed some evidence of improvement in motor activity in patients with PD.[12,25] However, the efficacy data being accounted for by a placebo response cannot be dismissed without a suitably powered controlled study. Furthermore, the magnitude of clinical responses observed suggests that the level of dopamine replacement offered by ProSavin may be suboptimal. Therefore, OXB-102 was designed to provide a higher level of dopamine replacement than ProSavin, to achieve a greater therapeutic effect. *In vitro* characterization of OXB-102 showed significantly higher levels of dopamine production compared with that of ProSavin in transduced human primary neurons.[24]

The design of the pre-clinical efficacy study was similar to that previously described, using localized delivery of vector to the most dopamine-depleted area of the striatum in order to maximize efficacy and avoid off-target dopaminergic adverse effects.[23] Since ProSavin was previously shown to cause almost complete reversal of motor activity in the MPTP primate model, it was used as a positive control for this study.[23] Given the difficulties in showing a dose response in this animal model without increasing group sizes significantly, the study aimed to evaluate two doses of OXB-102 only. These were considered the most likely doses to be evaluated clinically. The behavioral data show that OXB-102 resulted in comparable efficacy to ProSavin, both at a similar dose to ProSavin and also at a dose that was five times lower.

6-FMT PET imaging was performed to monitor the restoration of vector-mediated dopaminergic activity and to confirm that the behavioral effects observed were associated with dopamine replacement. The radioligand used, 6-FMT, was chosen over the classical radioligand fluoroDOPA, because it has a higher affinity for the AADC

enzyme and because it provides a more direct marker for vector-expressed AADC.[32] This radioligand has already been used to assess the conversion of L-Dopa to dopamine in patients with PD who received an AAV-AADC vector.[33] Additionally, in contrast to fluoro-DOPA, 6-FMT is not metabolized by catechol-O-methyltransferase in the periphery; thus, no radiometabolites enter the brain, which, in turn, increases the specific-to non-specific uptake.[32] Finally, it is assumed that long-term tissue trapping of decarboxylized 6-FMT occurs in the plasma and not the vesicular compartment.[34] The latter probably allowed visualization of vector-mediated AADC activity, in contrast to fluoroDOPA, which relies on vesicular trapping. Comparison with baseline scans clearly showed a depletion of AADC-mediated activity after MPTP intoxication that was consistent with the impaired motor performance observed in all of the study animals and that remained stable over time in the EIAV-Null control group. Conversely, the increase in AADC activity in the ProSavin and OXB-102 groups was consistent with the behavioral recovery observed. These findings and the lack of AADC activity recovery in EIAV-Null controls suggest that any increase in Ki post-vector administration was a likely result of vector-mediated AADC transgene expression. Furthermore, the higher levels of activity observed in the OXB-102 HD-treated group are in line with previous findings that showed significantly higher dopamine levels in human primary neurons transduced with OXB-102 compared to ProSavin.[24] Unfortunately, it was impossible to correlate *in vivo* improvements with post-mortem measurements, as no significant differences in the transduction volume of the three transgenes were observed across treatment groups. This is probably due to the strength of the antibody-target protein interaction. However, as previously demonstrated with the ProSavin vector,[23] we have used immunohistochemistry and RNAScope techniques to show co-expression of the *TH* and *AADC* genes in transduced striatal cells *ex vivo* and the functionality of the construct through behavioral and PET assessments *in vivo* in NHPs.

The GLP toxicology study was performed as part of the clinical development program for OXB-102 to support a regulatory submission. The safety profile was consistent with the pre-clinical and clinical studies for ProSavin[12,23] and demonstrates that protein expression from the optimized vector configuration, and subsequent increase in dopamine production, did not trigger any toxicological issues. The antibody responses reported are consistent with those previously observed in pre-clinical and clinical studies of EIAV-based gene therapy approaches—including the ProSavin phase I-II clinical trial, where anti-VSV-G (vesicular stomatitis virus G protein) and p26 responses were common—but responses against the therapeutic transgenes were not observed.[23] The biodistribution analysis suggests that OXB-102 was not found outside of the target area in the brain at any meaningful levels. These results are consistent with previous pre-clinical analyses of ProSavin.

In conclusion, the results achieved in these pre-clinical studies demonstrate the efficacy and safety of an enhanced dopaminergic lentiviral vector, OXB-102, and strongly support the clinical evaluation in patients with PD.

MATERIALS AND METHODS

Vector Production by Transient Transfection

The EIAV lentiviral vector system used to produce the EIAV vectors for the efficacy study involved the transient transfection of human embryonic 293T cells; methods were previously described.[34] The titers of the EIAV vectors used in the study were determined by integration (DNA) titer assay using a method previously described.[24]

For the GLP safety study, the OXB-102 vector was produced in a manner analogous to that for the GMP-grade clinical vector in which the vector-containing supernatant was harvested and the vector was purified and concentrated by anion exchange chromatography and hollow fiber technology. This method has been described previously.[35] Vector titer was determined by integration assay as described earlier.

Animals

The efficacy study was conducted in accordance with EU Directive 86/609/EEC and in compliance with the Standards for Humane Care and Use of Laboratory Animals of the Office of Laboratory Animal Welfare (OLAW no. A5826-01) in a facility authorized by local authorities (authorization no. B92-032-02). The experimental protocol was reviewed and approved (authorization no. A13_003) by the local ethics committee (CETEA no. 44). All efforts were made to minimize animal suffering, and animal care was supervised by veterinarians and animal technicians skilled in the health care and housing of NHPs. Sixteen adult male cynomolgus monkeys (Macaca fascicularis, supplied by Sicombrec, Makati, the Philippines) with a mean age of 2.5 years ± 0.1 years and a mean weight of 3.48 kg ± 0.1 kg were housed under standard environmental conditions (12-h:12-h light:dark cycle; temperature, 22°C ± 1°C; and humidity, 50%), with free access to food and water.

The GLP safety study was performed by Primetrics (Singapore) in accordance with the Organization for Economic Cooperation and Development (OECD) principles on GLP and the US Food and Drug Administration GLP for Nonclinical Laboratory Studies (Title 21 of the code of Federal Regulations, Part 58), with the exception of activity assessment using EthoVision and MRI procedures. Six male and six female healthy naive cynomolgus macaques (Macaca fascicularis), previously obtained from Nafovanny (Long Thanh, Vietnam), were acquired for use on the study. The animals were 3–5 years old and weighed 2.1–3.6 kg prior to commencement of dosing. The animals were drug naive at the initiation of the study. Animals were housed under standard conditions as described earlier.

MPTP Model

Parkinsonism was induced by intramuscular injections of 0.25 mg/kg of MPTP for 7 consecutive days, as previously described.[23] Cycles of MPTP intoxication were repeated until a significant and stable

reduction of spontaneous locomotor activity of at least 80% relative to baseline was sustained for over 1 month.

MRI

MRI was performed on all animals from both studies pre- and post-vector administration in order to allow precise determination of the coordinates for surgical administration, confirm correct placement post-administration, and also determine the regions of interest for PET analysis (efficacy study only).

For the efficacy study, animals were anesthetized by an intramuscular injection of ketamine (10 mg/kg) and xylazine (1 mg/kg) and placed in the magnet in a sphinx position, fixed by mouth and ear bars to a stereotactic MRI-compatible frame (M2E, Villepinte, France). Once in the magnet, animals were heated by a hot air flux, and their temperature and respiration parameters were monitored remotely. MRI was performed on a 7 Tesla horizontal scanner (Varian-Agilent Technologies, Palo Alto, CA, USA) equipped with a gradient coil reaching 100 millitesla per meter (mT/m; 300-μs rise time) and a circular radio frequency 1H surface coil (RAPID Biomedical, Rimpar, Germany). T2-weighted images were acquired using a high-resolution, two-dimensional (2D), fast spin-echo sequence (469 μm^2 × 469 μm^2 in-plane resolution, 1-mm slice thickness, 40 slices), with an effective echo time (TE) of 62 ms, a repetition time (TR) of 4,750 ms, and an acquisition time (Tacq) of 16 min. For T2*-weighted images, the parameters used were as follows: 469 μm^2 × 469 μm^2 in-plane resolution, 1-mm slice thickness, 40 slices, TE of 5 (from 5.5 to 30 ms), TR of 2 ms, and Tacq of 8 min.

For the GLP safety study, animals were pre-medicated with atropine sulfate (0.04–0.06 mg/kg intramuscularly [i.m.]) and anesthetized by an i.m. injection of ketamine (10 mg/kg). The animals were then positioned in an MRI-compatible stereotaxic frame (Kopf Instruments, Model 1430M) and then scanned in a Siemens 3-Tesla Magnetron Tim Trio MT imaging scanner (Siemens Medical Solutions, Erlangen, Germany). Three-dimensional magnetization-prepared rapid gradient echo (MP-RAGE) images were obtained with an isotropic voxel size of 0.5 × 0.5 × 0.5 mm.

Surgical Procedure

For both studies, animals were anesthetized as described earlier for MRI, and this was maintained with propofol (1 mg/kg/h) after endotracheal intubation (efficacy study only). Temperature was maintained at 37°C using a feedback-coupled heating blanket, and the respiratory rate, SpO2, EtCO2, cardiac rhythm, and blood pressure were continuously monitored.

Intracerebral injection of the vectors was performed with a Micro Pump and Micro4 Controller (World Precision Instruments, Sarasota, FL, USA) using a custom Hamilton blunt 28G, 50-mm-long sterile needle attached to a glass syringe, using a guide tube and a constant injection rate of 3 μL/min. Animals received bilateral injections of 50 μL test vector into two sites per hemisphere (efficacy study) or 100 μL test vector or buffer per hemisphere (safety study) into the post-commissural putamen. Post-operatively, analgesia was ensured by buprenorphine (0.01 mg/kg, i.m.) administration for three days.

Behavioral Assessments

For the efficacy study, a CRS scale was used to score the appearance and severity of parkinsonian symptoms as previously described.[23] Primates were assessed at baseline and then daily during the MPTP intoxication, weekly during the stabilization phases, and every 2–3 weeks thereafter. For activity assessments, all animals were videotaped for 40 min in a video cage on five separate occasions prior to MPTP intoxication in order to quantify baseline spontaneous locomotor activity, expressed as TDM, using EthoVision software (Noldus, the Netherlands). Animals were then filmed weekly during MPTP intoxication, during stabilization and for the first 3 months following vector administration, and once every 3 weeks thereafter.

For the safety study, activity (TDM) and dyskinesia rating were recorded 3 times prior to vector or buffer administration and once during weeks 4 and 13 and toward the end of the post-treatment observation. Activity over a 30-min period was assessed using the EthoVision system, and the dyskinesia rating was undertaken according to the revised Non-Human Primate Dyskinesia Rating Scale (NHPDysR).[36] Animals were also scored for behavioral effects at least twice weekly, commencing 1 week post-vector or -buffer administration until week 4 and weekly thereafter.

L-Dopa Challenge

Stably parkinsonian macaques received an acute systemic L-Dopa challenge prior to and at 3 months post-vector administration to evaluate their responsiveness to pharmacological dopaminergic treatment. Animals received a 20–30 mg/kg per oral administration (p.o.) dose of L-Dopa, preceded or followed by an off-medication control assessment. Locomotor activity was quantified over 6 h, as described earlier.

PET Scans

All study animals in the efficacy study received a 6-FMT scan at baseline, post-MPTP lesioning, and at 6 months post-vector administration.[37] Primates were anesthetized with an i.m. injection of ketamine (10 mg/kg) and xylazine (1 mg/kg), and anesthesia was maintained with propofol (1 mg/kg/h) throughout the imaging session. Animals were placed in a PET-dedicated stereotactic-like animal holder, with the head resting on a mouth bar, fixed by blunt ear bars. Throughout all imaging exams, temperature was maintained at 37°C using a feedback-coupled heating blanket, and the respiration rate, SpO2, EtCO2, cardiac rhythm, and blood pressure were continuously monitored. Ready-to-inject, >99% radiochemically pure 6-FMTyr radiotracer (6-[^{18}F] fluoro-L-m-tyrosine, Centre de Recherches du Cyclotron, Liège University, Belgium; 152.84 MBq ± 1.46 MBq) was injected intravenously at the start of data acquisition. Imaging was performed using a primate PET scanner, FOCUS 220 (Siemens, Munich, Germany), with a 1.5 mm axial resolution 4% sensitivity, a time coincidence window of 6 ns, and energy discrimination levels between 350 and 650 keV. Data were acquired for 90 min, and list mode data were

sorted in 26 frames. The attenuation correction factor was measured with an external 57Co source before radiotracer injection. The emission sinograms were normalized, corrected for attenuation and radioactivity decay, and reconstructed using Fourier rebinning (FORE) and ordered subset expectation maximization (OSEM) 2D (16 subsets and 4 iterations).

Quantitative parametric images were calculated with the Patlak graphical analysis method, using the cerebellum as a reference region that is void of any specific uptake of the radioligand. Subsequently, quantitative data were extracted from these parametric PET images by co-registering them with anatomical T2-weighted MRI images on which the regions of interest were manually determined around the injection sites in the putamen. The chosen quantification yielded parametric images or absolute values that reflect the enzymatic activity of AADC as measured by 6-FMTyr (i.e., Ki [min^{-1}]). The intensity-color scale of the parametric images correspond to a quantitative value of the measured biological parameter. Color scales were matched to allow comparison between the MPTP and the post-treated stages, thus avoiding the subjective manual adjustment of thresholds of intensity on individual images.

Statistical Analysis

Behavioral data were analyzed using repeated-measures ANOVA and Fisher's LSD post hoc correction. PET and immunohistochemical data were analyzed using a Student's t test or one-way ANOVA and a Fisher's LSD post hoc correction. Data are expressed as mean ± SEM.

Histology

Animals from the efficacy study were deeply anesthetized, and blood was collected. A lethal dose of pentobarbital was delivered before transcardial perfusion with 0.9% NaCl followed by 4% ice-cold paraformaldehyde (Sigma, St. Louis, USA). The brains were removed and post-fixed in 4% paraformaldehyde and then cryopreserved by immersion into sucrose-containing phosphate buffer gradients of increasing concentration (10%–20%). Brains were sliced into 40-μm-thick sections using a freezing microtome. Sections were first incubated in 1% H_2O_2 for 20 min and in PBS containing 4.5% normal goat serum and 0.2% Triton X-100 for 30 min. Sections were then incubated for 48 h at room temperature in PBS containing 0.2% Triton X-100, 3% normal serum, and the appropriate dilution of the primary antibody (according to the manufacturer's recommendation). The primary antibodies were directed against TH (Abcam, Cambridge, MA, USA), AADC (Millipore, Burlington, MA, USA), CH-1 (Invitrogen, Abingdon, UK), GFAP (DakoCytomation, Glostrup, Denmark), and NeuN (Millipore, Burlington, MA, USA). After incubation in the primary anti-serum, sections were processed using the avidin-biotin peroxidase method (VECTASTAIN Elite ABC Kit, Vector Laboratories). Sections were analyzed using an Axioskop 2 Plus microscope (Zeiss, Berlin, Germany) and/or confocal Nikon A1 Software NIS Element. In order to determine transduction volumes, the volume of the putamen was first determined for each animal on NeuN-stained sections spaced 1,280 μm apart and covering the entire putamen using Mercator software. Then, marker volumes were calculated from AADC-, TH-, or CH1-stained sections spaced 640 μm apart using the same software.

Th mRNA expression was determined using *in situ* hybridization (ISH) with the RNAScope V2 assay and RNAscope Probe – Hs-TH-C3 (Advanced Cell Diagnostics, Newark, CA, USA). Floating sections were rinsed in PBS and pretreated with RNAscope (Advanced Cell Diagnostics Newark, CA, USA) hydrogen peroxide solution for 10 min. Sections were then mounted on slides (Super-Frost Plus; Thermo Fisher Scientific, Waltham, MA, USA) and dried for 1 h at 60°C and then overnight at room temperature. Slides were pretreated with RNAscope Target Retrieval Reagent for 15 min at 100°C and protease-IV solution for 30 min at 40°C. Slides were then incubated with the Hs-TH-C3 probe for 30 min at 40°C. Hybridization signal was amplified and revealed at 40°C using the RNAscope Multiplex FL V2 and OPAL 650 reagent (Akoya Biosciences). Sections were then incubated in PBS containing 5% normal goat serum, 1 mg/mL BSA, and 0.2% Triton X-100 for 30 min and then for 24 h in PBS containing 0.2% Triton X-100, 3% normal serum, and AADC primary antibody (Millipore, Burlington, MA, USA) at the appropriate dilution (according to the manufacturer's recommendation). AADC immunostaining was revealed using Alexa-488-coupled secondary antibody. Sections were then counterstained with DAPI and analyzed using a Leica SP8 confocal microscope.

Western Blotting

For both studies, serum samples from each animal taken pre- and post-vector administration were evaluated for antibody responses against components of the OXB-102 vector or transgene products by western blot analysis and against non-reduced lysates from either untransfected HEK293T cells or HEK293T cell lysates that contained all components of OXB-102, ProSavin, and EIAV-Null vectors (VSVG, p26/GagPol, NeoPT, TH, AADC, and CH-1). Control antibodies included a polyclonal rat anti-VSVG antibody, a polyclonal rabbit anti-NeoPT antibody, and a mouse anti-p26 monoclonal antibody.

Biodistribution

From each animal in the safety study, samples of buffy coat were collected and analyzed at weeks 2 and 4, and plasma samples were collected and analyzed at week 2 post-treatment by qPCR or qRT-PCR analysis for vector presence. At the end of the study, full macro- and microscopic examinations were performed on a wide variety of tissues, and organ weights were measured. Additional tissue and fluid samples were also collected for vector presence outside the brain, and periodic blood sampling was performed throughout the study for western blot analysis of antibody responses against components of the OXB-102 vector or transgenes (discussed earlier). A full clinical chemistry and urine analysis was also performed on samples obtained pre- and post-vector or buffer administration.

Toxicology

The assessment of toxicity against OXB-102 was based on mortality, clinical signs, body weight, and qualitative food consumption. In

addition, in-life assessments were performed by ophthalmoscopy, electrocardiography, and blood pressure measurement.

Histopathology

At the end of the 26-week post-treatment observation period, all animals in the safety study were euthanized by intravenous pentobarbital sodium overdose preceded by ketamine sedation. External and internal examinations were performed before removal of any organs. A standard post-mortem examination was then performed, and abnormalities were recorded. Organs were weighed, and tissues were collected and fixed in neutral buffered formalin for histological processing and evaluation.

SUPPLEMENTAL INFORMATION

Supplemental Information can be found online at https://doi.org/10.1016/j.omtm.2019.07.002.

AUTHOR CONTRIBUTIONS

Conceptualization: S.P., P.H., and K.A.M.; Formal Analysis: R.A.B., N.V.C., and M.K.; Investigation: M.K., J.L., H.S., R.A.B., N.V.C., C.J., P.G., A.F., J.G., C.R., K.H., and S.P.; Resources: P.H. and K.A.M.; Writing – Original Draft: R.A.B., S.P., and G.S.R.; Writing – Review & Editing: K.B., J.L., M.K., H.S., G.S.R., Y.L., K.A.M., N.V.C., C.J., and P.H.; Supervision: K.B., Y.L., J.L., K.A.M., S.P., and P.H.; Project Administration: R.A.B.

CONFLICTS OF INTEREST

As this work was funded by Oxford Biomedica (OXB; UK), all OXB employees have a financial interest in the development of the gene therapy, which has entered a clinical trial.

ACKNOWLEDGMENTS

This work was funded by OXB (UK) Ltd. and the French National Research Agency (ANR DopaGene project ANR-13-PRTS-0012). This work was conducted in Fontenay-aux-Roses, France, and at Primetrics, 10 Science Park Road, Singapore Science Park II, Singapore 117684, Singapore.

REFERENCES

1. Guttman, M., Kish, S.J., and Furukawa, Y. (2003). Current concepts in the diagnosis and management of Parkinson's disease. CMAJ *168*, 293–301.
2. Rao, S.S., Hofmann, L.A., and Shakil, A. (2006). Parkinson's disease: diagnosis and treatment. Am. Fam. Physician *74*, 2046–2054.
3. Lee, H.M., and Koh, S.B. (2015). Many faces of Parkinson's disease: non-motor symptoms of Parkinson's disease. J. Mov. Disord. *8*, 92–97.
4. Kelberman, M.A., and Vazey, E.M. (2016). New pharmacological approaches to treating non-motor symptoms of Parkinson's disease. Curr. Pharmacol. Rep. *2*, 253–261.
5. Dauer, W., and Przedborski, S. (2003). Parkinson's disease: mechanisms and models. Neuron *39*, 889–909.
6. Gerfen, C.R., and Surmeier, D.J. (2011). Modulation of striatal projection systems by dopamine. Annu. Rev. Neurosci. *34*, 441–466.
7. Riederer, P., Lange, K.W., and Youdim, M.B. (1993). Recent advances in pharmacological therapy of Parkinson's disease. Adv. Neurol. *60*, 626–635.
8. Sit, S.Y. (2000). Dopamine agonists in the treatment of Parkinson s disease past, present and future. Curr. Pharm. Des. *6*, 1211–1248.
9. Olanow, C.W., and Stocchi, F. (2018). Levodopa: a new look at an old friend. Mov. Disord. *33*, 859–866.
10. Marsden, C.D. (1994). Problems with long-term levodopa therapy for Parkinson's disease. Clin. Neuropharmacol. *17* (*Suppl 2*), S32–S44.
11. Cenci, M.A. (2014). Presynaptic Mechanisms of l-DOPA-Induced Dyskinesia: The Findings, the Debate, and the Therapeutic Implications. Front. Neurol. *5*, 242.
12. Palfi, S., Gurruchaga, J.M., Ralph, G.S., Lepetit, H., Lavisse, S., Buttery, P.C., Watts, C., Miskin, J., Kelleher, M., Deeley, S., et al. (2014). Long-term safety and tolerability of ProSavin, a lentiviral vector-based gene therapy for Parkinson's disease: a dose escalation, open-label, phase 1/2 trial. Lancet *383*, 1138–1146.
13. Piguet, F., Alves, S., and Cartier, N. (2017). Clinical gene therapy for neurodegenerative diseases: past, present, and future. Hum. Gene Ther. *28*, 988–1003.
14. Lin, J.Y., Xie, C.L., Zhang, S.F., Yuan, W., and Liu, Z.G. (2017). Current experimental studies of gene therapy in Parkinson's disease. Front. Aging Neurosci. *9*, 126.
15. Wang, L., Muramatsu, S., Lu, Y., Ikeguchi, K., Fujimoto, K., Okada, T., Mizukami, H., Hanazono, Y., Kume, A., Urano, F., et al. (2002). Delayed delivery of AAV-GDNF prevents nigral neurodegeneration and promotes functional recovery in a rat model of Parkinson's disease. Gene Ther. *9*, 381–389.
16. Gasmi, M., Herzog, C.D., Brandon, E.P., Cunningham, J.J., Ramirez, G.A., Ketchum, E.T., and Bartus, R.T. (2007). Striatal delivery of neurturin by CERE-120, an AAV2 vector for the treatment of dopaminergic neuron degeneration in Parkinson's disease. Mol. Ther. *15*, 62–68.
17. Marks, W.J., Jr., Ostrem, J.L., Verhagen, L., Starr, P.A., Larson, P.S., Bakay, R.A., Taylor, R., Cahn-Weiner, D.A., Stoessl, A.J., Olanow, C.W., and Bartus, R.T. (2008). Safety and tolerability of intraputaminal delivery of CERE-120 (adeno-associated virus serotype 2-neurturin) to patients with idiopathic Parkinson's disease: an open-label, phase I trial. Lancet Neurol. *7*, 400–408.
18. Marks, W.J., Jr., Bartus, R.T., Siffert, J., Davis, C.S., Lozano, A., Boulis, N., Vitek, J., Stacy, M., Turner, D., Verhagen, L., et al. (2010). Gene delivery of AAV2-neurturin for Parkinson's disease: a double-blind, randomised, controlled trial. Lancet Neurol. *9*, 1164–1172.
19. Warren Olanow, C., Bartus, R.T., Baumann, T.L., Factor, S., Boulis, N., Stacy, M., Turner, D.A., Marks, W., Larson, P., Starr, P.A., et al. (2015). Gene delivery of neurturin to putamen and substantia nigra in Parkinson disease: A double-blind, randomized, controlled trial. Ann. Neurol. *78*, 248–257.
20. Kaplitt, M.G., Feigin, A., Tang, C., Fitzsimons, H.L., Mattis, P., Lawlor, P.A., Bland, R.J., Young, D., Strybing, K., Eidelberg, D., and During, M.J. (2007). Safety and tolerability of gene therapy with an adeno-associated virus (AAV) borne GAD gene for Parkinson's disease: an open label, phase I trial. Lancet *369*, 2097–2105.
21. LeWitt, P.A., Rezai, A.R., Leehey, M.A., Ojemann, S.G., Flaherty, A.W., Eskandar, E.N., Kostyk, S.K., Thomas, K., Sarkar, A., Siddiqui, M.S., et al. (2011). AAV2-GAD gene therapy for advanced Parkinson's disease: a double-blind, sham-surgery controlled, randomised trial. Lancet Neurol. *10*, 309–319.
22. Azzouz, M., Martin-Rendon, E., Barber, R.D., Mitrophanous, K.A., Carter, E.E., Rohll, J.B., Kingsman, S.M., Kingsman, A.J., and Mazarakis, N.D. (2002). Multicistronic lentiviral vector-mediated striatal gene transfer of aromatic L-amino acid decarboxylase, tyrosine hydroxylase, and GTP cyclohydrolase I induces sustained transgene expression, dopamine production, and functional improvement in a rat model of Parkinson's disease. J. Neurosci. *22*, 10302–10312.
23. Jarraya, B., Boulet, S., Ralph, G.S., Jan, C., Bonvento, G., Azzouz, M., Miskin, J.E., Shin, M., Delzescaux, T., Drouot, X., et al. (2009). Dopamine gene therapy for Parkinson's disease in a nonhuman primate without associated dyskinesia. Sci. Transl. Med. *1*, 2ra4.
24. Stewart, H.J., Ralph, G.S., Fong-Wong, L., Strickland, I., McCloskey, L., Barnes, L., Blount, I., Wells, O., Truran, C.J., Kingsman, A.J., et al. (2016). Optimizing transgene configuration and protein fusions to maximize dopamine production for the gene therapy of Parkinson's disease. Hum. Gene Ther. Clin. Dev. *27*, 100–110.
25. Palfi, S., Gurruchaga, J.M., Lepetit, H., Howard, K., Ralph, G.S., Mason, S., Gouello, G., Domenech, P., Buttery, P.C., Hantraye, P., et al. (2018). Long-term follow-up of a phase I/II study of ProSavin, a lentiviral vector gene therapy for Parkinson's disease. Hum. Gene Ther. Clin. Dev. *29*, 148–155.
26. Goetz, C.G., Wuu, J., McDermott, M.P., Adler, C.H., Fahn, S., Freed, C.R., Hauser, R.A., Olanow, W.C., Shoulson, I., Tandon, P.K., and Leurgans, S.;

Parkinson Study Group (2008). Placebo response in Parkinson's disease: comparisons among 11 trials covering medical and surgical interventions. Mov. Disord. *23*, 690–699.

27. Keitel, A., Wojtecki, L., Hirschmann, J., Hartmann, C.J., Ferrea, S., Südmeyer, M., and Schnitzler, A. (2013). Motor and cognitive placebo-/nocebo-responses in Parkinson's disease patients with deep brain stimulation. Behav. Brain Res. *250*, 199–205.

28. Mittermeyer, G., Christine, C.W., Rosenbluth, K.H., Baker, S.L., Starr, P., Larson, P., Kaplan, P.L., Forsayeth, J., Aminoff, M.J., and Bankiewicz, K.S. (2012). Long-term evaluation of a phase I study of AADC gene therapy for Parkinson's disease. Hum. Gene Ther *23*, 377–381.

29. Cederfjäll, E., Sahin, G., Kirik, D., and Björklund, T. (2012). Design of a single AAV vector for coexpression of TH and GCH1 to establish continuous DOPA synthesis in a rat model of Parkinson's disease. Mol. Ther *20*, 1315–1326.

30. Christine, C.W., Bankiewicz, K.S., Van Laar, A.D., Richardson, R.M., Ravina, B., Kells, A.P., Boot, B., Martin, A.J., Nutt, J., Thompson, M.E., and Larson, P.S. (2019). Magnetic resonance imaging-guided phase 1 trial of putaminal AADC gene therapy for Parkinson's disease. Ann. Neurol *85*, 704–714.

31. Marks, W.J., Jr., Baumann, T.L., and Bartus, R.T. (2016). Long-term safety of patients with Parkinson's disease receiving rAAV-2-Neutrurin (CERE-120) gene transfer. Hum. Gene Ther *27*, 522–527.

32. Eberling, J.L., Bankiewicz, K.S., O'Neil, J.P., and Jagust, W.J. (2008). PET 6-[F]fluoro-L-m-tyrosine studies of dopaminergic function in human and nonhuman primates. Front. Hum. Neurosci. *1*, 9.

33. Mittermeyer, G., Christine, C.W., Rosenbluth, K.H., Baker, S.L., Starr, P., Larson, P., Kaplan, P.L., Forsayeth, J., Aminoff, M.J., and Bankiewicz, K.S. (2012). Long-term evaluation of a phase 1 study of AADC gene therapy for Parkinson's disease. Hum. Gene Ther. *23*, 377–381.

34. Brown, W.D., DeJesus, O.T., Pyzalski, R.W., Malischke, L., Roberts, A.D., Shelton, S.E., et al. (1999). Localization of trapping of 6-[(18)F]fluoro-L-m-tyrosine, an aromatic L-amino acid decarboxylase tracer for PET. Synapse *34*, 111–123.

35. Binley, K., Widdowson, P., Loader, J., Kelleher, M., Iqball, S., Ferrige, G., de Belin, J., Carlucci, M., Angell-Manning, D., Hurst, F., et al. (2013). Transduction of photoreceptors with equine infectious anemia virus lentiviral vectors: safety and biodistribution of StarGen for Stargardt disease. Invest. Ophthalmol. Vis. Sci. *54*, 4061–4071.

36. Fox, S.H., Johnston, T.H., Li, Q., Brotchie, J., and Bezard, E. (2012). A critique of available scales and presentation of the Non-Human Primate Dyskinesia Rating Scale. Mov. Disord. *27*, 1373–1378.

37. Lemaire, C., Libert, L., Franci, X., Genon, J.L., Kuci, S., Giacomelli, F., and Luxen, A. (2015). Automated production at the curie level of no-carrier-added 6-[(18)F]fluoro-L-dopa and 2-[(18)F]fluoro-L-tyrosine on a FASTlab synthesizer. J. Labelled Comp. Radiopharm. *58*, 281–290.